Acta Crystallographica Section B
Structural Science
ISSN 0108-7681

Structures of stable and metastable $Ge_2Sb_2Te_5$, an intermetallic compound in GeTe–Sb_2Te_3 pseudobinary systems

Toshiyuki Matsunaga,[a]* Noboru Yamada[b] and Yoshiki Kubota[c]

[a]Characterization Technology Group, Matsushita Technoresearch, Inc., 3-1-1 Yagumo-Nakamachi, Moriguchi, Osaka 570-8501, Japan, [b]Storage Media Systems Development Center, Matsushita Electric Industrial Co., Ltd, 3-1-1 Yagumo-Nakamachi, Moriguchi, Osaka 570-8501, Japan, and [c]Department of Environmental Sciences, Faculty of Science, Osaka Women's University, 2-1 Daisen-cho, Sakai, Osaka 590-0035, Japan

Correspondence e-mail: matsunaga.toshiyuki@jp.panasonic.com

Received 31 May 2004
Accepted 14 September 2004

The most widely used memory materials for rewritable phase-change optical disks are the GeTe–Sb_2Te_3 pseudobinary compounds. Among these compounds, $Ge_2Sb_2Te_5$ crystallizes into a cubic close-packed structure with a six-layer period (metastable phase) in the non-thermal equilibrium state, and a trigonal structure with a nine-layer period (stable phase) in the thermal equilibrium state. The structure of the stable phase has Ge/Sb layers in which Ge and Sb are randomly occupied, as does the structure of the metastable phase, while the conventionally estimated structure had separate layers of Ge and Te. The metastable and stable phases are very similar in that Te and Ge/Sb layers stack alternately to form the crystal. The major differences between these phases are: (i) the stable phase has pairs of adjacent Te layers that are not seen in the metastable phase and (ii) only the metastable phase contains vacancies of *ca* 20 at. % in the Ge/Sb layers.

1. Introduction

The pseudobinary compound GeTe–Sb_2Te_3 is known as the most widely used material for rewritable phase-change optical recording media, such as digital versatile disk–random access memory (DVD–RAM). In a thermal equilibrium state this system has three intermetallic compounds: $Ge_2Sb_2Te_5$, $GeSb_2Te_4$ and $GeSb_4Te_7$ (Abrikosov & Danilova-Dobryakova, 1965). These three compounds can be described as structures with cubic close-packing periodicity (...*ABCABC*...), where the stacking rules of the Ge, Sb and Te layers are different from each other. $Ge_2Sb_2Te_5$, $GeSb_2Te_4$ and $GeSb_4Te_7$ have nine- ($P\bar{3}m1$), 21- ($R\bar{3}m$) and 12-layer ($R\bar{3}m$) structures, respectively (Petrov *et al.*, 1968; Agaev & Talybov, 1966). In addition, GeTe and Sb_2Te_3 are described as six- (Goldak *et al.*, 1966) and 15-layer (Wyckoff, 1986) structures. However, recording films of this pseudobinary material crystallize through instantaneous heating/cooling by laser irradiation into a single metastable phase with an NaCl-type structure ($Fm\bar{3}m$) over a wide composition range of GeTe from 100 mol% to at least 50 mol% (Yamada, 2000). In this structure the Cl:4(*a*) site is completely occupied by Te atoms, whereas the Na:4(*b*) site is randomly occupied by Ge and Sb atoms and by vacancies. When the composition of the pseudobinary compound is expressed as $(GeTe)_x + (Sb_2Te_3)_{1-x}$ $(0 \leq x \leq 1)$, the ratio of the vacancy continuously changes according to $(1 - x)/(3 - 2x)$.

Petrov *et al.* (1968) and Kooi & De Hosson (2002) examined the stable phase of $Ge_2Sb_2Te_5$ with an electron transmission microscope and reported that Ge, Sb and Te formed their respective layers to construct a nine-layered trigonal structure in a stacking manner of the cubic closest packing. The two sets

Table 1
Refined structural parameters for the $Ge_2Sb_2Te_5$ metastable phase at room temperature.

The space group is $Fm\bar{3}m$. Standard deviations are shown in parentheses. The final R factors and lattice parameter are $R_{wp} = 0.0414$, $R_p = 0.0295$, $R_I = 0.0114$, R_{wp} expected = 0.0153 and $a = 6.0293$ (1) Å.

Atom	Site	g	x	y	z	B (Å^2)
Te	4(*a*)	1.0	0	0	0	1.48 (1)
$Ge_{0.5}Sb_{0.5}$	4(*b*)	0.784 (2)	1/2	1/2	1/2	3.54 (3)

of authors showed, however, completely opposite results for the site occupation of Ge and Sb atoms. In this work we scrutinized the crystal structure of this stable phase by powder X-ray diffraction using SPring-8, a synchrotron radiation facility, and found that Ge and Sb do not independently occupy their respective sites or layers, but they in fact randomly occupy both sites or layers. As we already clarified, in the crystal of the $GeSb_2Te_4$ stable phase, Ge and Sb are not located in separate layers, but in Ge/Sb layers in which the two elements are randomly arranged. In this work we also reexamined the metastable $Ge_2Sb_2Te_5$ structure for comparison with its stable phase and reported the structural analysis results for these two phases.

2. Experimental

The specimen used for diffraction measurement was obtained by the following method. First, a thin film of $Ge_2Sb_2Te_5$, approximately 3000 Å thick, was sputtered onto a glass disk with a 120 mm diameter. Inductively coupled plasma (ICP) atomic-emission spectrometry confirmed that the composition of the specimen was close to $Ge_2Sb_2Te_5$. The film was amorphous just after its formation. It was crystallized by laser irradiation into a metastable phase. The film was then powdered by scraping with a spatula and the powder was packed in a quartz capillary tube with an internal diameter of 0.2 mm. To insulate against the atmosphere, the opening of the capillary was melted shut with an oxyacetylene flame. After diffraction experiments for the metastable phase, the powder specimen was heated to 823 K and annealed for 5 min, which treatment resulted in transformation to the stable phase.

A diffraction experiment was performed at room temperature using the BL02B2 beamline at the Japan Synchrotron Radiation Research Institute (SPring-8; Nishibori *et al.*, 2001). A precollimator mirror and a double-crystal monochromator were used to ensure that the incident beam utilized for the diffraction experiments was highly monochromatic and parallel. The energies of the incident beam were 29.435 keV ($\lambda = 0.41955$ Å) for the powdered specimen of the metastable phase and 29.452 keV ($\lambda = 0.42151$ Å) for the stable phase. Intensity data were collected using a Debye–Scherrer camera with a 287 mm radius. An imaging plate with a pixel area of 100 μm^2 was used as the detector. The angular resolution was 0.02°. High-temperature experiments were also performed while nitrogen gas, set at specified temperatures, was blown onto the capillary tube exposing the specimen for 5 min at each temperature. The mean heating or cooling rate from measurement to measurement was 10 K min^{-1}. The crystal structures were refined using the Rietveld method (Rietveld, 1969). The program used was *RIETAN* (Izumi & Ikeda, 2000). To improve the accuracy of the Rietveld analyses, intensity data in increments of 0.01° were obtained by reading the imaging plate for a pixel area of 50 μm^2. The energy of the synchrotron radiation used was confirmed by recording the diffraction intensity of CeO_2 ($a = 5.4111$ Å) powder as a reference specimen at room temperature under the same conditions.

3. Results

3.1. Crystal structure of the metastable phase

We previously analyzed the crystal structure of the $Ge_2Sb_2Te_5$ metastable phase in detail (Yamada & Matsunaga, 2000). This time another precise analysis was performed to compare with the stable phase. The structural analysis results are shown in Table 1 and Fig. 1. The metastable phase belongs to the space group $Fm\bar{3}m$ (Hahn, 1995). Among three types of elements, Te occupied 100% of the 4(*a*) site, while Ge and Sb randomly occupied the 4(*b*) site forming an NaCl-type structure. The 4(*b*) site was not filled with atoms, leaving vacancies of *ca* 20 at. %, to retain the ratio of Ge + Sb:Te = 4:5. To confirm the number of vacancies, the g parameter of the 4(*b*) site (site occupation rate of $Ge_{0.5}Sb_{0.5}$) was made variable. The result was that g was almost 0.8, as shown in Table 1. The mean volume per single atom is *ca* 30.7 Å^3.

3.2. Crystal structure of the stable phase

The stable phase of $Ge_2Sb_2Te_5$ has already been analyzed by Petrov *et al.* (1968). First we made a Rietveld analysis according to this structure model (Table 2 [A]). However, no

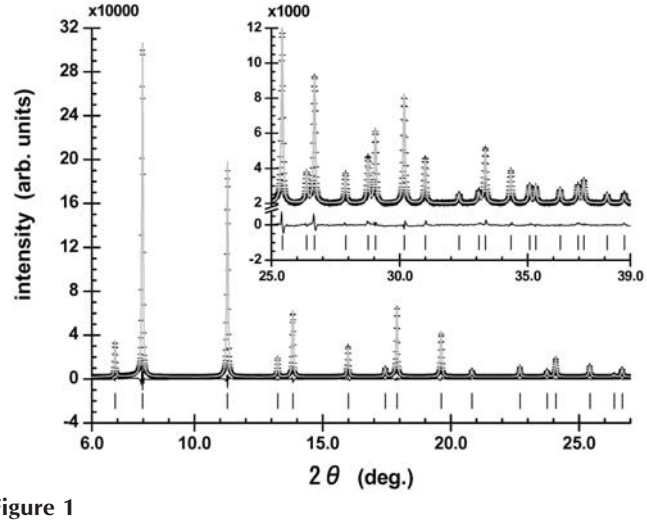

Figure 1
Observed (+) and calculated (gray line) X-ray diffraction profiles of the $Ge_2Sb_2Te_5$ metastable phase at room temperature (300 K). A difference curve (observed − calculated) appears at the bottom of each figure; under the curve, reflection markers are indicated by vertical spikes.

Table 2
Structural parameters for [A] $Ge_2Sb_2Te_5$ shown by Petrov *et al.* (1968) and for [B] by Kooi & De Hosson (2002).

The space group is $P\bar{3}m1$: a = 4.20, c = 16.96 Å.

[A] atom	Site	x	y	z	[B] atom
Te1	1(*a*)	0	0	0	Te1
Sb	2(*d*)	2/3	1/3	0.106	Ge
Te2	2(*d*)	1/3	2/3	0.212	Te2
Ge	2(*c*)	0	0	0.317	Sb
Te3	2(*d*)	2/3	1/3	0.421	Te3

satisfactory results were obtained (R_{wp} = 0.0803, R_I = 0.0270). The next analysis, performed according to Kooi & De Hosson's (2002) model (Table 2 [B]), produced better results (R_{wp} = 0.0743, R_I = 0.0212) than the model of Petrov *et al.* (1968). However, a difference between the measured (I_o) and calculated (I_c) intensities still remained, especially with weaker diffraction peaks. We have already analyzed in detail the structure for $GeSb_2Te_4$, an intermetallic compound of the GeTe–Sb_2Te_3 pseudobinary system (Matsunaga & Yamada, 2004). The results revealed that Ge and Sb did not independently occupy each specific site, but existed randomly across both sites. Then, the random occupation of Ge and Sb between the 2:2(*d*) and 4:2(*c*) sites (see Table 3) was also assumed for $Ge_2Sb_2Te_5$. That is to say, the analysis was performed regarding $g_{Sb}^{2:2d}$ as an independent variable and assuming the following between both sites:

$$g_{Ge}^{2:2d} = 1 - g_{Sb}^{2:2d},\ g_{Sb}^{4:2c} = 1 - g_{Sb}^{2:2d} \text{ and } g_{Ge}^{4:2c} = 1 - g_{Sb}^{4:2c}, \quad (1)$$

where $g_{Sb}^{2:2d}$ represents the occupation rate of Sb at the 2:2(*d*) site. As seen in Table 3 and Fig. 2, this assumption produced satisfactory analytical results. The mean volume per single atom was *ca* 29.6 Å^3.

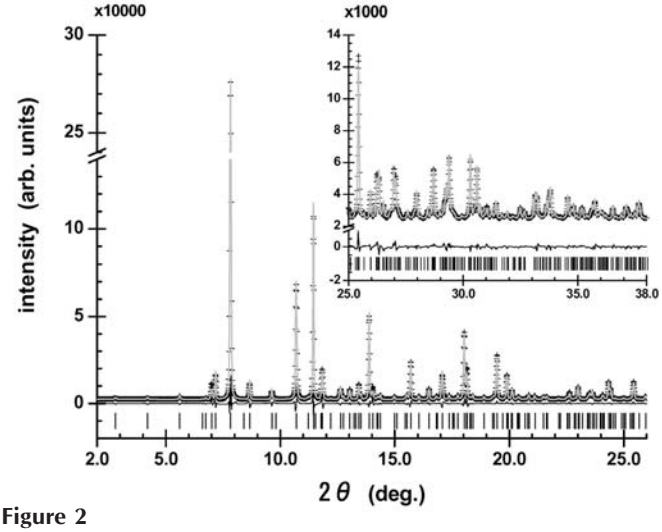

Figure 2
Observed (+) and calculated (gray line) X-ray diffraction profiles of the $Ge_2Sb_2Te_5$ stable phase at room temperature (300 K). A difference curve (observed − calculated) appears at the bottom of each figure; under the curve, reflection markers are indicated by vertical spikes.

Table 3
Refined structural parameters for the $Ge_2Sb_2Te_5$ stable structure at room temperature.

The space group is $P\bar{3}m1$. Standard deviations are shown in parentheses. The final R factors and lattice parameters are R_{wp} = 0.0603, R_p = 0.0392, R_I = 0.0108, R_{wp} expected = 0.0151, and a = 4.2247 (1), c = 17.2391 (4) Å.

Atom	Site	g	x	y	z	B (Å^2)
Te1	1: 1(*a*)	1.0	0	0	0	1.16 (9)
Ge/Sb1	2: 2(*d*)	0.559/0.441 (11)	2/3	1/3	0.1061 (3)	1.80 (6)
Te2	3: 2(*d*)	1.0	1/3	2/3	0.2065 (2)	0.67 (6)
Ge/Sb2	4: 2(*c*)	0.441/0.559	0	0	0.3265 (2)	1.87 (9)
Te3	5: 2(*d*)	1.0	2/3	1/3	0.4173 (1)	1.47 (7)

3.3. Temperature dependence of the crystal structure

It is common knowledge that when the $Ge_2Sb_2Te_5$ metastable phase is heated, its structure transforms into a stable phase around 500 K, showing an exothermic peak in the differential scanning calorimetry (DSC) curve (Yamada *et al.*, 1991). The temperature dependence of the structural parameters for the stable phase obtained by high-temperature measurements is shown in Table 4. The diffraction measurement temperatures were controlled as 673 → 773 → 823 → 873 → 923 → 300 K. The parameters were determined by the Rietveld method at each temperature. As seen in this table, at temperatures of 673 and 773 K, a small amount of metastable phase still remained in the stable phase. However, above 823 K the powder specimen was entirely transformed into a stable structure as a single phase and the g parameters were locked at constant values. When the temperature was raised further, a very small quantity of the NaCl-type structure emerged again at 923 K and coexisted with the stable phase, probably for the following reason. This temperature is located near the boundary of the following two regions in the phase diagram of the GeTe–Sb_2Te_3 pseudobinary system (Abrikosov & Danilova-Dobryakova, 1965): one is the $Ge_2Sb_2Te_5$ single-phase region and the other is the liquid and GeTe high-temperature phase (NaCl-type structure) coexisting region. In addition to this high-temperature experiment, another experiment was carried out using a new powder specimen. The diffraction measurement temperatures were programmed as 723 → 798 → 653 → 453 → 353 K. The analyzed structural parameters, shown in Table 4, indicate that the atomic position z of each variable site in the crystal structure of the stable phase is almost constant, regardless of temperature. The Ge/Sb ratio is also invariant, as is the structure of $GeSb_2Te_4$ (Matsunaga & Yamada, 2004). Table 4 shows that in this experiment, the $Ge_2Sb_2Te_5$ powdered specimen was in a single stable phase at least between 798 and 873 K. We therefore annealed a metastable powder specimen at 823 K to make it a single stable phase and performed a precise X-ray diffraction measurement at room temperature.

It is presumed that the specimens at 673, 723 and 773 K were in a quasi-thermal equilibrium state just after the transition from a metastable to a stable phase. We expected that

Table 4
Temperature dependences of structural parameters for the $Ge_2Sb_2Te_5$ powdered specimen.

Standard deviations are shown in parentheses. The last column shows the mass fractions of phases with stable and NaCl-type structures contained in the specimen.

Atom site parameter	Ge/Sb1 2:2(*d*) g_{Ge}/ g_{Sb}	Ge/Sb1 2:2(*d*) *z*	Te2 3:2(*d*) *z*	Ge/Sb2 4:2(*c*) *z*	Te3 5:2(*d*) *z*	Mass fractions Stable/NaCl
673 K	0.46/0.54 (3)	0.1054 (8)	0.2081 (4)	0.3292 (6)	0.4171 (5)	0.95/0.05
773 K	0.54/0.46 (2)	0.1060 (4)	0.2065 (2)	0.3277 (3)	0.4174 (2)	0.98/0.02
823 K	0.59/0.41 (2)	0.1059 (4)	0.2064 (2)	0.3277 (3)	0.4182 (3)	1.0/0.0
873 K	0.59/0.41 (1)	0.1066 (3)	0.2058 (2)	0.3274 (2)	0.4168 (2)	1.0/0.0
923 K	0.59/0.41 (3)	0.1071 (8)	0.2065 (5)	0.3282 (5)	0.4147 (4)	0.94/0.06
300 K	0.58/0.42 (2)	0.1068 (6)	0.2062 (3)	0.3260 (4)	0.4164 (3)	0.99/0.01
723 K	0.50/0.50 (2)	0.1058 (4)	0.2077 (3)	0.3277 (3)	0.4176 (3)	0.98/0.02
798 K	0.54/0.46 (2)	0.1058 (4)	0.2067 (2)	0.3278 (3)	0.4176 (2)	1.0/0.0
653 K	0.55/0.45 (2)	0.1062 (3)	0.2068 (2)	0.3273 (3)	0.4171 (2)	1.0/0.0
453 K	0.55/0.45 (1)	0.1061 (3)	0.2064 (2)	0.3268 (2)	0.4175 (2)	1.0/0.0
353 K	0.55/0.45 (1)	0.1062 (4)	0.2067 (2)	0.3267 (2)	0.4174 (2)	1.0/0.0

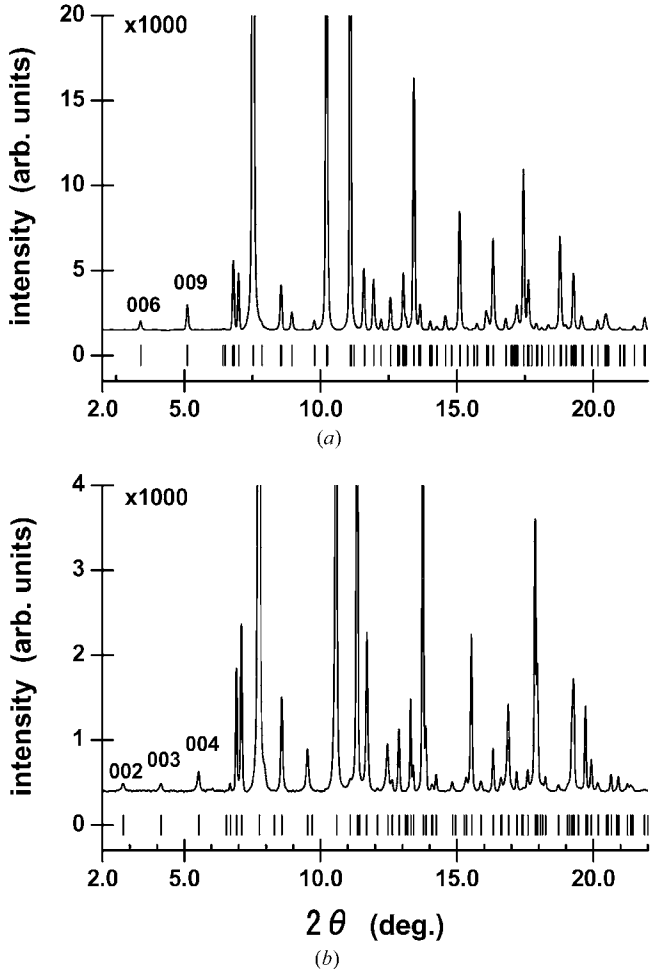

Figure 3
Diffraction patterns of $GeSb_2Te_4$ (top) and $Ge_2Sb_2Te_5$ (bottom) measured respectively at 823 K. Reflection markers are indicated by vertical spikes under the patterns of each figure. No metastable phase peaks are observed in their patterns.

the phase transition would be completed by annealing for a sufficient time at each temperature.

4. Discussion

Fig. 3 shows the diffraction pattern of the $Ge_2Sb_2Te_5$ stable phase taken at 823 K, together with that of $GeSb_2Te_4$. Some weak but sharp Bragg peaks, which appeared depending on the length of the stacking period, are observed in the low-angle side of the patterns (002, 003 and 004 for $Ge_2Sb_2Te_5$, 006 and 009 for $GeSb_2Te_4$). From these patterns, it can be assumed that $Ge_2Sb_2Te_5$ contained few structures with other periods including $GeSb_2Te_4$; in other words, the majority or all of the $Ge_2Sb_2Te_5$ powdered specimen crystallized in its specific structure as a single phase.

The $Ge_2Sb_2Te_5$ stable phase has a nine-layered trigonal structure in which each layer is shifted from the next by 1/3 in the $[\bar{1}10]$ direction. According to the crystal structure shown by Petrov *et al.* (1968), the layer stacking is expressed by

$$[\mathrm{A}]: \frac{\mathrm{Te}}{a}\cdot\frac{\mathrm{Sb}}{b}\cdot\frac{\mathrm{Te}}{c}\cdot\frac{\mathrm{Ge}}{a}\cdot\frac{\mathrm{Te}}{b}\cdot\frac{\mathrm{Te}}{c}\cdot\frac{\mathrm{Ge}}{a}\cdot\frac{\mathrm{Te}}{b}\cdot\frac{\mathrm{Sb}}{c}\cdot\frac{\mathrm{Te}}{a}.$$

On the other hand, according to Kooi & De Hosson (2002) the stacking is

$$[\mathrm{B}]: \frac{\mathrm{Te}}{a}\cdot\frac{\mathrm{Ge}}{b}\cdot\frac{\mathrm{Te}}{c}\cdot\frac{\mathrm{Sb}}{a}\cdot\frac{\mathrm{Te}}{b}\cdot\frac{\mathrm{Te}}{c}\cdot\frac{\mathrm{Sb}}{a}\cdot\frac{\mathrm{Te}}{b}\cdot\frac{\mathrm{Ge}}{c}\cdot\frac{\mathrm{Te}}{a}.$$

A comparison of these expressions revealed that Ge and Sb were reversed. However, according to our analysis, Ge and Sb were distributed across both 2(*c*) and 2(*d*) sites. The ratio of Ge and Sb was different between the sites; a site dependency in the occupation rate was found (see Table 3). As shown in Table 2, the dependency inclines toward the [B] model. To confirm the accuracy of the determined *g* value, we performed Rietveld analyses in which the value of *g* was fixed from 0 to 1 at intervals of 0.1 and the other parameters were variable. The results are shown in Fig. 4. The curve in the figure is a quadratic function fitted by the least-squares method; R_{wp} shows the bottom at $g = 0.45$.

The metastable NaCl-type structure in the hexagonal notation is a six-layered structure in which alternate stacks of Te and Ge/Sb layers are accumulated infinitely along the *c*-axis (Fig. 5*a*). On the other hand, the stable phase has a nine-layer structure in which NaCl blocks are stacked along the *c* axis (Fig. 5*b*). An NaCl block is formed by alternately laminating Te and Ge/Sb until nine layers and both the head and tail of a block always end with a Te layer. The interatomic distance is shown in Table 5. In the metastable phase the distance is fixed at 3.012 Å for every atomic pair in the crystal. In the stable phase it is distributed from 2.898 to 3.753 Å and in particular, the Te—Te distance between the neighboring two NaCl blocks is markedly longer than the others. This distance is close to the

Table 5
Interatomic distances (Å) in stable $Ge_2Sb_2Te_5$ at room temperature.

Te1—Ge/Sb1 × 6	3.0487 (28)
Ge/Sb1—Te2 × 3	2.9911 (31)
Ge/Sb1—Te1 × 3	3.0487 (28)
Te2—Ge/Sb1 × 3	2.9911 (31)
Te2—Ge/Sb2 × 3	3.1983 (26)
Ge/Sb2—Te3 × 3	2.8975 (21)
Ge/Sb2—Te2 × 3	3.1983 (26)
Te3—Ge/Sb2 × 3	2.8975 (21)
Te3—Te3 × 3	3.7533 (26)

sum of the Te^{2-} ion radii (2.07 Å × 2) shown by Shannon (1976).

We conducted the following analysis to examine the bonding state of Te—Te. To simplify the calculation, the structure model of [B] was first employed and the electron density was analyzed by the molecular orbital method (DV-*Xa* method). The *SCAT* program was used (Adachi *et al.*, 1978). The origin of the calculation was set at the center of 5:Te3 (2/3, 1/3, 0.41726) − 5′:Te3 (1/3, 2/3, 0.58274); that is at (1/2, 1/2, 1/2) (see Figs. 5*b* and 6). The calculation was conducted by configuring a cluster with 24 atoms that exist within the range of r = 5.5 Å. The result is shown in Figs. 7(*a*) and (*b*) for the plane, including Te5 and Te5′ in the unit cell (the shaded plane in Fig. 6) and the plane of z = 1/2, respectively. As seen in these figures, almost no localized electron peak is found that reveals covalent bonding between Te atoms in adjacent layers. The bond overlap population between the two atoms, which shows the number of electrons that contribute to the covalent bond between them, was calculated to be 0.007, which means that the population is almost zero. This supports the above result. The net (effective) charge, which indicates the number of excess electrons that an atom has received from other atoms in a cluster, was calculated for both Te atoms to be *ca* +0.02 (+ means positive charge). This suggests that this Te—Te pair has little ionic bond nature. When a similar calculation was performed with the structure model [A], the bond-overlap population was also almost zero (0.008) and the net charge was −0.02. From these facts we believe that the two adjacent Te layers are neither ionically bonded nor covalently bonded, but connected with metallic or van der Waals bonding. Fig. 8 shows an electron density distribution (wR = 0.032, R = 0.033) in the $Ge_2Sb_2Te_5$ stable phase obtained by Maximum Entropy Method (MEM) analysis (Takata *et al.*, 2001). The MEM

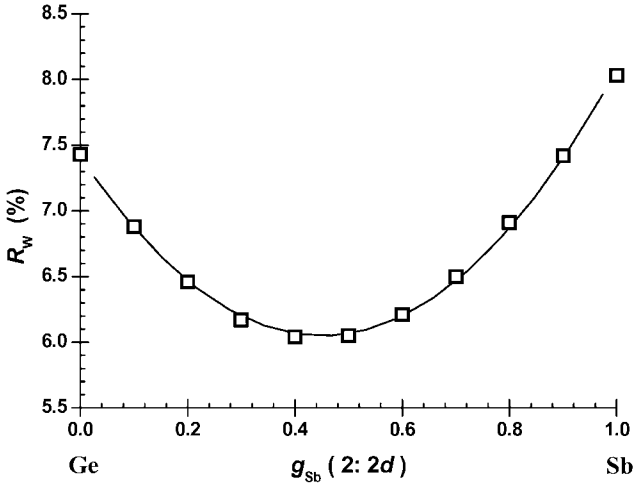

Figure 4
Agreement factor R_{wp} as a function of the ratio of the Ge/Sb mixture between 2:2(*d*) and 4:2(*c*) sites for refinements with fixed values of the parameter g at the 2:2(*d*) site at intervals of 0.1 from 0.0 to 1.0.

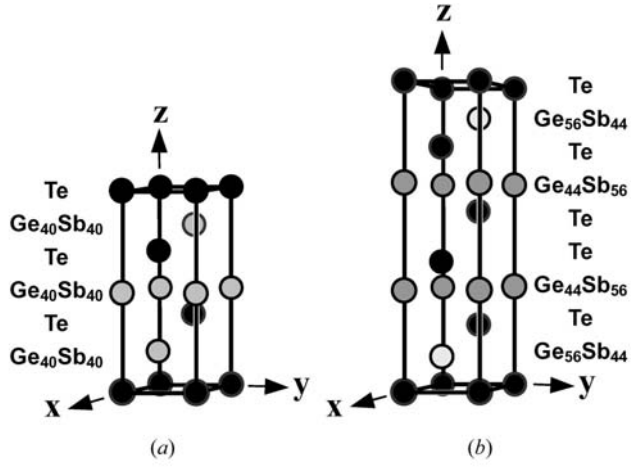

Figure 5
Crystal structures of (*a*) metastable and (*b*) stable $Ge_2Sb_2Te_5$, shown schematically in perspective. Black circles show the atomic positions for Te. Gray circles show those for Ge or Sb.

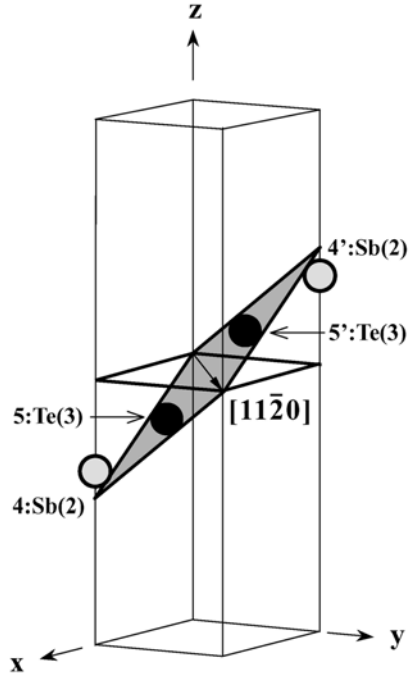

Figure 6
Schematic drawing of planes where the molecular orbital and MEM calculations were performed. One is the plane of z = 1/2; the other is the plane containing two Te atoms, 5:Te3 and 5′:Te3, shown by black circles. 4:Sb4 and 4′:Sb4 are over and under this plane, respectively.

calculation was performed by the computer program *ENIGMA* (Tanaka *et al.*, 2002). While in the MEM analysis results the distribution reflects the crystal symmetry, the results of the molecular orbital method reveal an isotropic distribution, which probably reflects that the calculation was conducted on a small atomic cluster. In spite of such differences and the peak height being a little uneven, both analyses show a similar electron distribution, supporting the validity of calculations using the molecular orbital method.

5. Conclusion

$Ge_2Sb_2Te_5$ in the metastable phase crystallizes into a six-layer cubic close-packed (NaCl-type) structure in which the Ge/Sb and Te layers are stacked alternately. The Ge/Sb layer in the metastable phase contains as much as 20 at. % vacancies, which makes the structure very sparse spatially. Therefore, the mean volume per single atom is larger than that of the stable phase. On the other hand, in the stable phase Te and Ge/Sb are stacked alternately nine times to form an NaCl block and then the blocks are stacked to construct a nine-layered trigonal structure with cubic close-packed stacking. Te layers cover both ends of a block. In addition, the stable phase has no vacancy in the Ge/Sb layer, unlike the metastable phase. The structures of the metastable phase and the stable phase, however, are similar to each other; fundamentally Te and Ge/Sb are stacked alternately. Another common feature is that Ge and Sb are randomly arranged to make the Ge/Sb layer. The major structural differences are only whether Te—Te layers exist in the stacking and whether the Ge/Sb layers contain vacancies.

The synchrotron radiation experiments were performed on BL02B2 at SPring-8 with the approval of the Japan Synchrotron Radiation Research Institute (JASRI) (Proposal No. 2003 A0478-ND1-np). We express our sincere gratitude to K. Kato and Dr M. Takata at JASRI, and Dr E. Nishibori and Professor M. Sakata at the Department of Applied Physics at Nagoya University for their advice on the experiment and its analysis. The electron density maps in Fig. 8 were drawn using a program named *Limner* produced by Y. Shimizu and H.

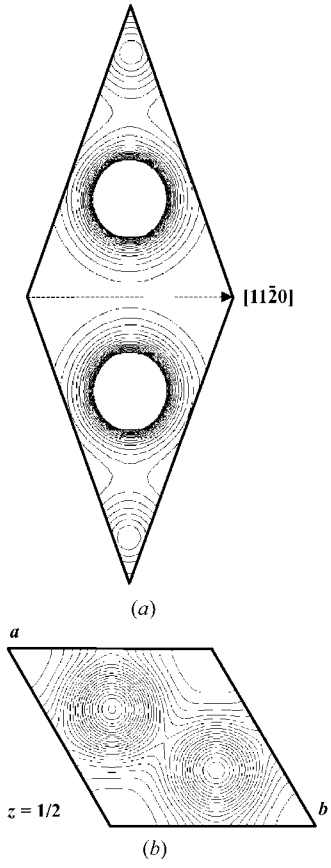

Figure 7
Electron density maps for the $Ge_2Sb_2Te_5$ stable phase obtained by calculation using the molecular orbital (DV-Xα) method (*a*: top) on a plane containing 5:Te3 and 5′:Te3, and (*b*: bottom) on the *c* plane at z = 1/2 in the unit cell shown in Fig. 5. Contours are drawn at intervals of 0.1 from 0.0 to 2.0 e Å^{-3} and at 0.01 from 0.0 to ∞ e Å^{-3}, respectively. The highest point in the latter map is *ca* 0.21–0.22 e Å^{-3} at the two peaks of (x, y) = (2/3, 1/3) and (1/3, 2/3).

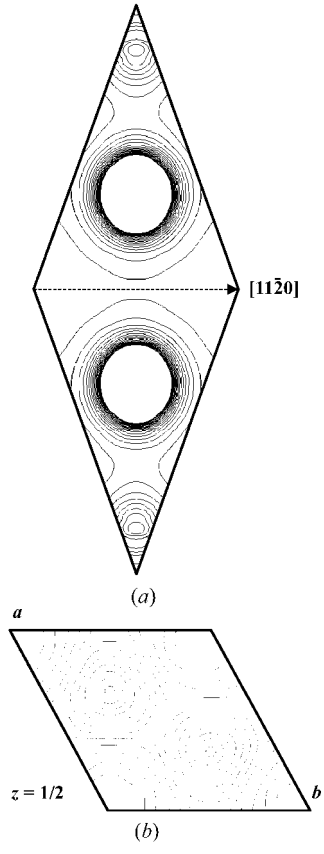

Figure 8
Electron density maps for the $Ge_2Sb_2Te_5$ stable phase obtained by MEM (*a*: top) on the plane containing 5:Te3 and 5′:Te3, and (*b*: bottom) on the *c* plane at z = 1/2 in the unit cell shown in Fig. 5. Contours are drawn at intervals of 0.1 from 0.0 to 2.0 e Å^{-3} and at 0.01 from 0.0 to ∞ e Å^{-3}, respectively. The highest point in the map is *ca* 0.12 e Å^{-3} at two peaks of (x, y) = (2/3, 1/3) and (1/3, 2/3).

Tanaka of Shimane University. We are indebted to them for allowing us to use their program. We thank Dr H. Tanaka and Dr M. Takata for the computer program *ENIGMA* for the MEM analysis.

References

Abrikosov, N. Kh. & Danilova-Dobryakova, G. T. (1965). *Izv. Akad. Auk. SSSR Neorg. Mater.* **1**, 204–207.
Adachi, N., Tsukada, N. & Satoko, C. (1978). *J. Phys. Soc. Jpn*, **45**, 875–883.
Agaev, K. A. & Talybov, A. G. (1966). *Sov. Phys. Crystallogr.* **11**, 400–402.
Goldak, J., Barrett, C. S., Innes, D. & Youdelis, W. (1966). *J. Chem. Phys.* **44**, 3323–3325.
Hahn, T. (1995). *International Tables for Crystallography*, Vol. A, Dordrecht: Kluwer Academic Publishers.
Izumi, F. & Ikeda, T. (2000). *Mater. Sci. Forum*, **321–324**, 198–203.
Kooi, B. J. & De Hosson, J. Th. M. (2002). *J. Appl. Phys.* **92**, 1, 3584–3590.
Matsunaga, T. & Yamada, N. (2004). *Phys. Rev. B*, **69**, 10, 104111, 1–8.
Nishibori, E., Takata, M., Kato, K., Sakata, M., Kubota, Y., Aoyagi, S., Kuroiwa, Y., Yamakata, M. & Ikeda, N. (2001). *Nucl. Instrum. Methods A*, **467–468**, 1045–1048.
Petrov, I. I., Imamov, R. M. & Pinsker, Z. G. (1968). *Sov. Phys. Crystallogr.* **13**, 339–342.
Rietveld, H. M. (1969). *J. Appl. Cryst.* **2**, 65–71.
Shannon, R. D. (1976). *Acta Cryst.* A**32**, 751–767.
Takata, M., Nishibori, E. & Sakata, M. (2001). *Z. Kristallogr.* **216**, 71–86.
Tanaka, H., Takata, M., Nishibori, E., Kato, K., Iishi, T. & Sakata, M. (2002). *J. Appl. Cryst.* **35**, 282–286.
Wyckoff, R W. G. (1986). *Crystal Structures*, Vol. 2. Malabar: Krieger.
Yamada, N. (2000). Kyoto University Doctoral Dissertation, Vol. 11 (in Japanese).
Yamada, N. & Matsunaga, T. (2000). *J. Appl. Phys.* **88**, 7020–7028.
Yamada, N., Ohno, E., Nishiuchi, K., Akahira, N. & Takao, M. (1991). *J. Appl. Phys.* **69**, 1, 2849–2856.